

New Concept for High Efficiency and Ultra-Low Emission Surface Combustor-Heater Using a Cyclic Flow Reversal Combustion Technology

S. Jugjai

Combustion and Engine Research Laboratory (CERL)
Department of Mechanical Engineering, Faculty of Engineering,
King Mongkut's University of Technology Thonburi
91 Prachauthit Road (Suksawad 48) Bangmod, Tungkru District,
Bangkok 10140
Tel: 0-2470-9128, Fax: 0-2470-9111
E-mail: sumrueng.jug@kmutt.ac.th

(Received : 1 December 2003 – Accepted : 1 July 2004)

Abstract: Research on a new surface combustor-heater (SCH) equipped cyclic flow reversal combustion (CFRC) technique was explored. Possible maximum thermal efficiency with favorable emission characteristics was pursued through furnace modifications and using past experience. Based on the existing experimental apparatus, modification was made in accordance with two hypotheses. A well-controlled boundary condition at the ends of the packed bed combustor could improve furnace thermal efficiency. Type of the packed bed may play a vital role

in improving furnace efficiency. Combustor performance was examined and evaluated. Some important operating parameters were clarified. Merits of this kind of combustor were also suggested. Results show that the additional flame traps play an important role in maintaining the boundary condition of the packed bed, whilst improving thermal efficiency. An increase in the thermal efficiency from 40 % to 66 % with a drastic reduction in CO from 700 ppm to 170 ppm and NO_x from 32 ppm to 14 ppm was achieved as compared with the previous data. Desirable trapezoidal temperature profiles were achieved by increasing the size of the alumina sphere (d_p) from about 5 mm to 16 mm. Mass flow rate of the cooling water of the tube bank strongly affects thermal efficiency and emission characteristics. Thermal input appreciably affects thermal efficiency but moderately affects the CO and NO_x emissions. CFRC can yield almost twice as much thermal efficiency as conventional one-way flow combustion (OWFC) with much smaller CO and NO_x emissions (as low as 30 ppm at 0 % O₂). CFRC is suitable for relatively lean combustion with significantly high thermal efficiency and low CO and NO_x emission. This SCH with CFRC concept can provide the basis for development of state-of-the-art technology for new versions and more advanced thermal systems, such as highly efficient ultra-low-pollutant-emission boilers, water heaters and steam super heaters for future efficient utilization of energy in both industrial and residential applications.

Keywords: Surface-combustor heater (SCH); Cyclic flow reversal combustion (CFRC); Ultra-low-pollutant emission; Boilers; Water heater; Packed bed.

Introduction

With the advent of CFRC [1] and SCH [2], the new SCH equipped with the concept of CFRC was first proposed by Jugjai et al. [3, 4]. Considerable practical benefits of the new SCH as compared with the conventional OWFC were revealed [3, 4]. These include a more favorable flame stabilization with extended flammability, a more uniform temperature profile in the combustion chamber with higher heat transfer performance and a much smaller emission of CO and NO_x. Nevertheless, further improvement in the thermal efficiency of the new SCH can be obtained by changing the boundary conditions of the packed bed and by changing the type of packed bed as suggested by Jugjai et al. [4]. This becomes the main topic of the present study.

The objective of this study is to further develop a new version of the SCH equipped with CFRC with some modifications at the packed bed and its boundary condition. Transient behavior under the modification of the system is observed. Improvements in thermal efficiency and emission characteristics are judged by comparing results with the previous data [4]. Effects of some important parameters such as, mass flow rate of the cooling water at the tube bank ($m_{w_{tb}}$) and

the heat input (CL) are clarified. Performance of the CFRC is assessed by making a comparison with those of the conventional OWFC through temperature profiles, thermal efficiencies and emission characteristics.

Experimental Apparatus and Procedure

Figure 1 shows an experimental apparatus of the recently developed new version of the SCH. The design concept, operational function, experimental apparatus and instrumentation are quite similar to those of the previous one [4]. However, some modifications were made in three areas. Firstly, the present apparatus consists totally of a randomly packed bed of solid alumina spheres, not partially consisting of the spheres at the tube bank with a stack of pieces of rectangular honeycomb porous ceramic plates flanged on both ends as in the previous apparatus [4]. Secondly, the diameter d_p of the alumina sphere is increased from 5 mm to 16 mm so as to increase the pore size and to reduce flame quenching during its propagation inside the packed bed. Thirdly, two flame traps have been included, as shown in Figure 2, each one installed at either end of the packed bed to minimize radiative heat loss and to prevent the flame from being pushed out of the packed bed. The flame traps also serve as heat exchangers in which the useful heat can be extracted from the supplied cooling water.

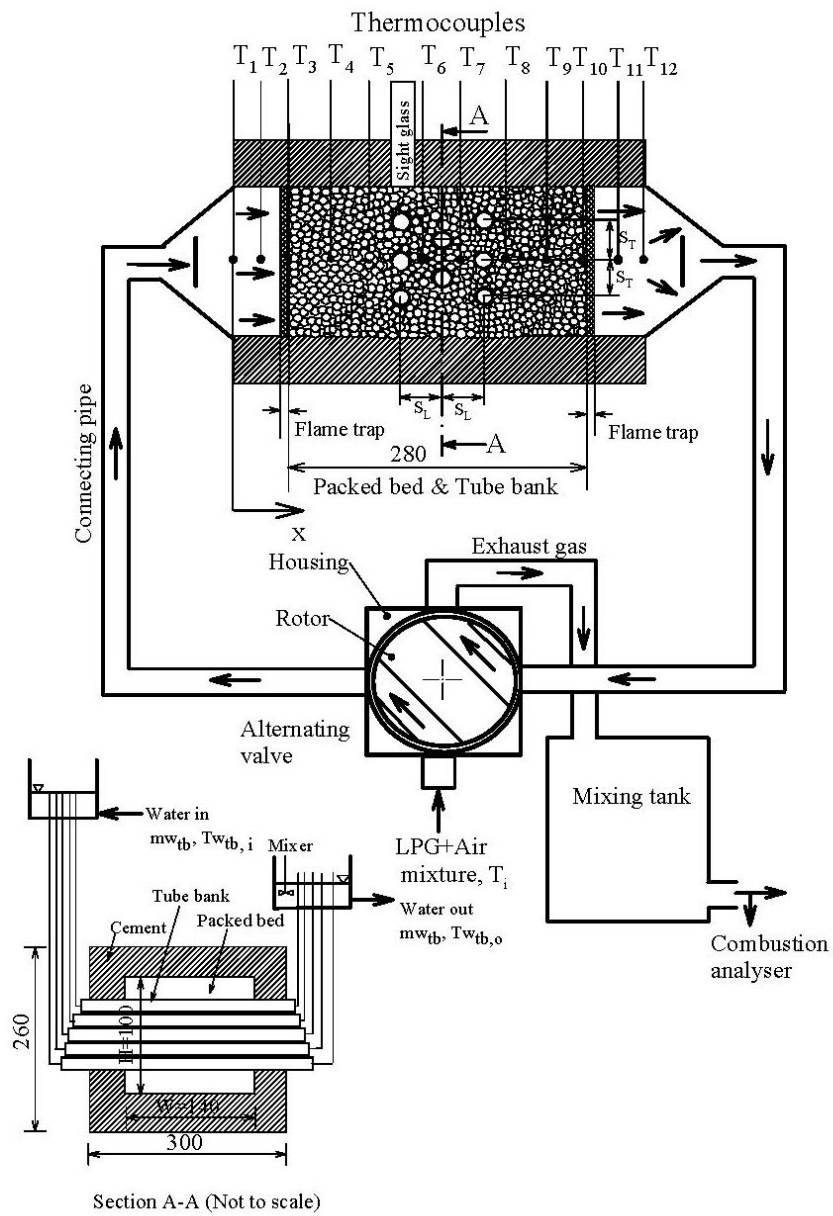


Figure 1. Experimental apparatus.

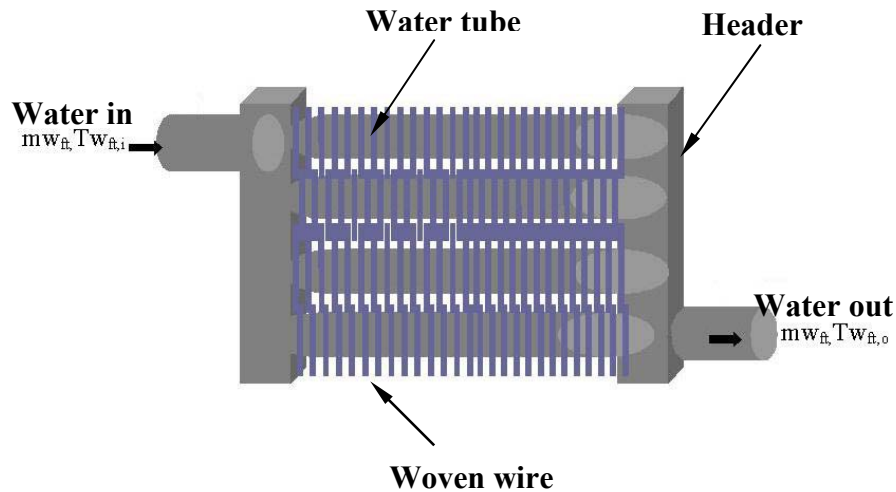


Figure 2. Flame trap.

To allow very high temperature measurement (up to 1800°C), B-type sheath thermocouples T_1 to T_{12} of wire diameter 0.5 mm were used. Other quantities, such as inlet and outlet bulk temperatures of the cooling water in the tube bank and in the flame traps, water mass flow rate, fuel mass flow rate, combustion air mass flow rate as well as gas temperatures and emission of CO and NO_x are still measured by the same equipment as in the previous study [4]. A quasi-steady state condition of CFRC was reached once the constant amplitude and the constant average over a half-period (t_{hp}) of the fluctuation temperatures T_1 to T_{12} were obtained. The operating procedures of the burner for both CFRC and OWFC are quite similar to those of the previous study [4] and the detailed explanation is omitted here.

In the current study, the heat transfer performance is judged by total thermal efficiency of the system (η_{tot}), which is defined as a summation of the thermal efficiency at the tube bank and at the frame traps as shown by equation (1),

$$\eta_{\text{tot}} = \eta_{\text{tb}} + \eta_{\text{ft}} \quad (1)$$

where η is defined as the ratio of the rate of heat transferred to the water in the tube bank or to the flame traps to the total heat supplied (CL) of the system. The combustion characteristics are evaluated from the measured NO_x and CO concentrations at the exit of the mixing tank, which is used for maintaining stable emission levels. The numerical value of the important quantities obtained from the experiment are summarized in Table 1.

Table 1. Operating conditions.

<u>Quantity</u>	<u>Value</u>
Average diameter of alumina sphere, d_p	5, 16 mm
Bed height, H	100 mm
Bed width, W	140 mm
Bed length, L	280 mm
Cooling water mass flow rate at tube bank, mw_{tb}	2.7–7.6 kg/min
Cooling water mass flow rate at flame trap, mw_{ft}	2x 0.88–2x 1.56 kg/min
Equivalence ratio, Φ	0.38–0.49 for the CFRC 0.49–0.79 for the OWFC

Half-period, t_{hp}	10–45	s
Inlet cooling water temperature, $T_{w_{ft,i}}$, $T_{w_{tb,i}}$	303	K
Inlet gas temperature, T_i	303	K
Longitudinal pitch, S_L	30	mm
Low heating value of LPG	115	MJ/m ³ [normal]
Number of tubes of tube bank	8	
Thermal input, CL	8.08–18.10	kW
Transverse pitch spacing, S_T	30	mm
Tube inside diameter, D_i	9	mm
Tube outside diameter, D_o	13.5	mm

Results

1. Effect of the flame traps on boundary condition, thermal efficiency and emission characteristics.

Effect of the flame traps on the boundary condition at both ends of the packed bed can be studied by comparing transient temperature profiles as shown in Figures 3 and 4, though different experimental conditions were used. With the flame trap (Figure 4), amplitude of the temperature swing at both ends of the packed bed was significantly reduced as compared to the setup without flame traps (Figure 3) obtained from the previous work [4]. Upon changing the flow direction from the backward flow to the forward flow in the two systems (without and with the flame trap), the inlet temperature change with time t from $t = 0$ to $t = t_{hp}$ has shown an opposite trend.

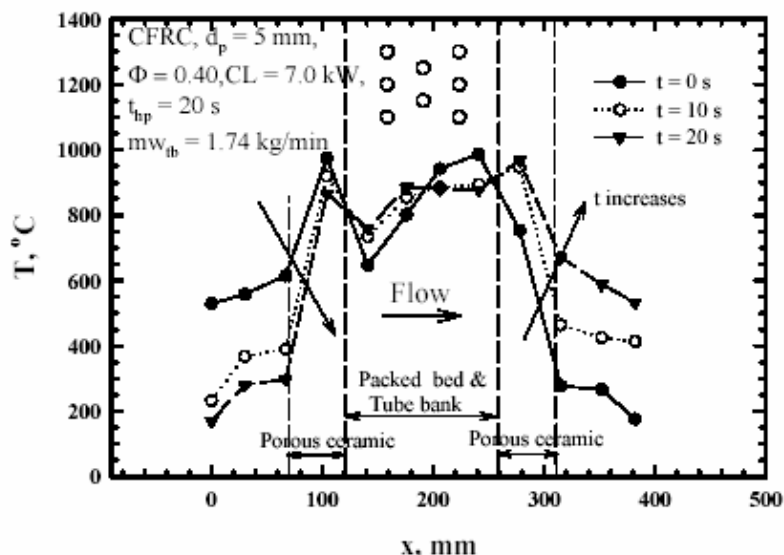


Figure 3. Typical transient temperatures of the CFRC (without flame trap).

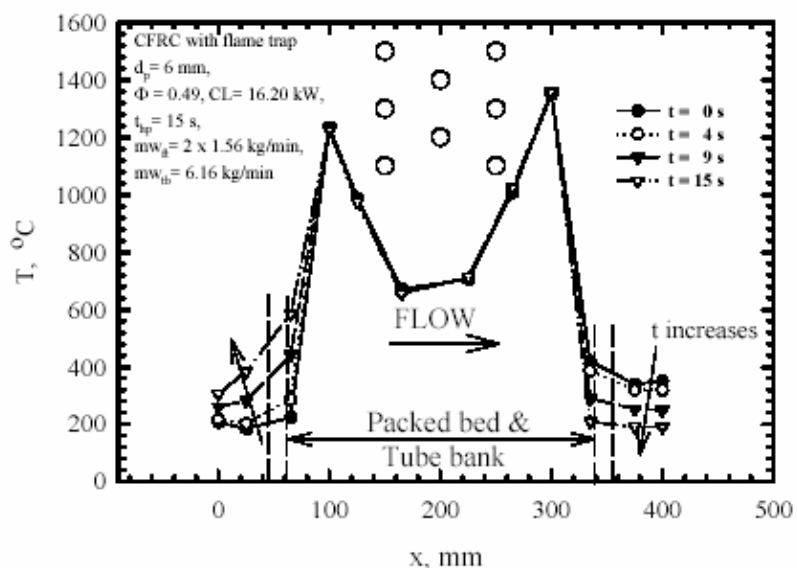


Figure 4. Typical transient temperatures of the CFRC (with flame trap).

Without the flame trap (Figure 3), the hot zone deep inside the packed bed from the inlet is strongly quenched by the in-flowing cool mixture resulting in a decrease in the temperature. On the other hand, a more stable hot zone at relatively high temperature level with an increase in the inlet temperature with time t was achieved with flame traps (Figure 4). With the flame trap, concave temperature profiles with two hot zones were observed because of a strong quenching effect by the tube bank and the flame traps. In spite of the concave temperature profiles, higher thermal efficiency η_{tot} with significantly lower CO and NO_x emission than those of the system without the flame traps were achieved as shown in Figure 5. The flame trap system yields maximum thermal efficiency $\eta_{\text{tot}} = 66\%$ with small amount of CO = 170 ppm and NO_x = 14 ppm, whereas the system without the flame trap yields maximum $\eta_{\text{tot}} = 40\%$ with relatively high CO and NO_x emission of about 700 ppm and 32 ppm, respectively. Thus, the flame trap system yielded 26% higher thermal efficiency with more complete combustion with extremely low NO_x emission as compared with the system without flame traps.

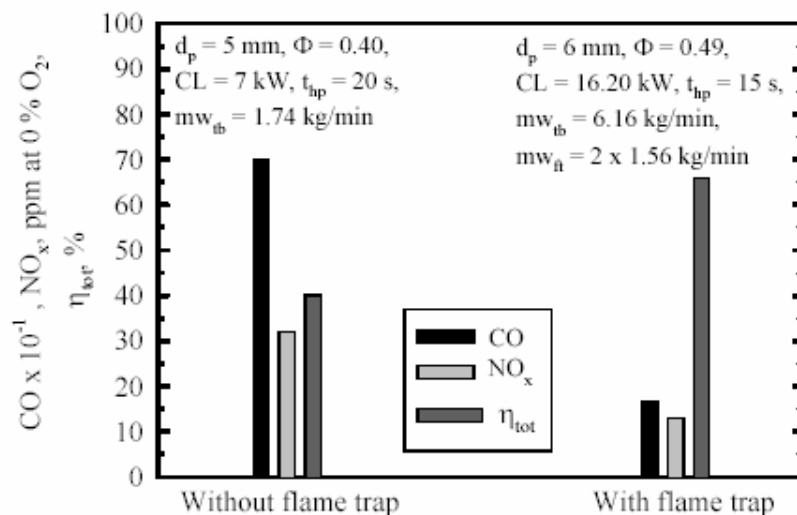


Figure 5. Comparison of CO, NO_x and η_{tot} between with- and without flame trap.

2. Effect of mass flow rate of the cooling water at the tube bank, mw_{tb} .

Size of the alumina sphere (d_p) was increased from 6 mm to 16 mm before variation in mw_{tb} was made. Because of the transient nature, temperatures of the CFRC were averaged over a half-period (t_{hp}) before making further explanations. Desirable trapezoidal, single hot zone and time-averaged temperature profiles at an interval t_{hp} (T_{av}) were achieved at $d_p = 16 \text{ mm}$ and other experimental conditions as specified in Figure 6. However, these desirable temperature profiles depend on mw_{tb} . Within the range $mw_{tb} = 3.4\text{-}6.16 \text{ kg/min}$, trapezoidal temperature profiles with the maximum temperature of T_6 were achieved.

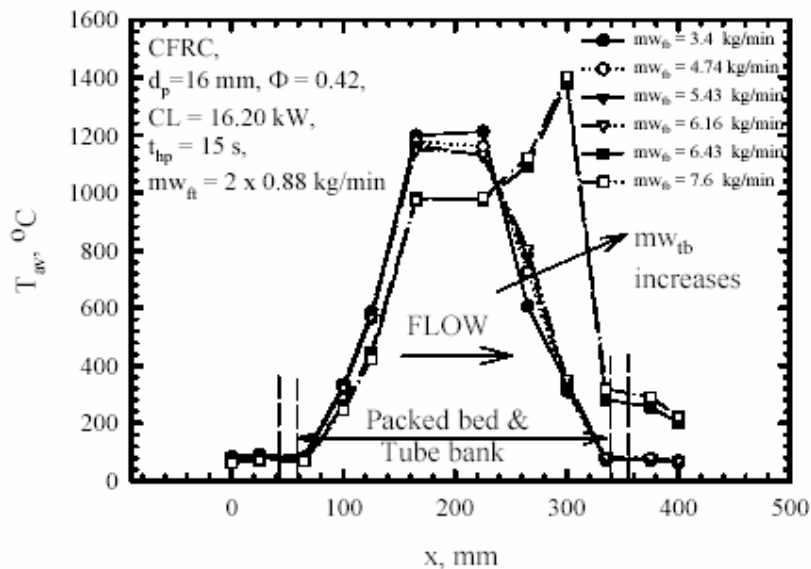


Figure 6. Effect of mw_{tb} on time averaged temperature profiles T_{av} .

In spite of the strong quenching effect, the hot zone can coincide with the tube bank. This phenomenon is very important in view of combustion and heat transfer. The combustion temperature can be significantly reduced because heat is removed simultaneously with the combustion process, and thus formation of nitrogen oxides is suppressed. Heat transfer to the tube bank can be greatly enhanced by thermal radiation emitted from the hot solid particles, leading to an increase in η_{tot} as shown in Figure 7 and a decrease in CO and NO_x as shown in Figure 8. However, at a certain value of mw_{tb} , i. e. $mw_{tb} = 6.43$ kg/min, unsymmetrical temperature profile was yielded and the maximum temperature zone shifted far away from the tube bank as shown in Figure 6, causing a drastic decrease in η_{tot} . Flame quenching by the tube bank was also significantly

reduced with the unsymmetrical flame shape resulting in a drastic decrease in CO emission with an increase in mw_{tb} as shown in Figure 8. η_{ft} has a small contribution to η_{tot} so long as the temperature profile becomes symmetrical (trapezoidal). In spite of the unsymmetrical temperature profile, η_{ft} could be significantly increased by increasing the water flow rate mw_{ft} of the flame trap located on the same side as the hot zone shifted. This provides an optional means for maintaining high total thermal efficiency η_{tot} . It is interesting to note that the NO_x emission of less than 40 ppm was observed throughout the experimental range.

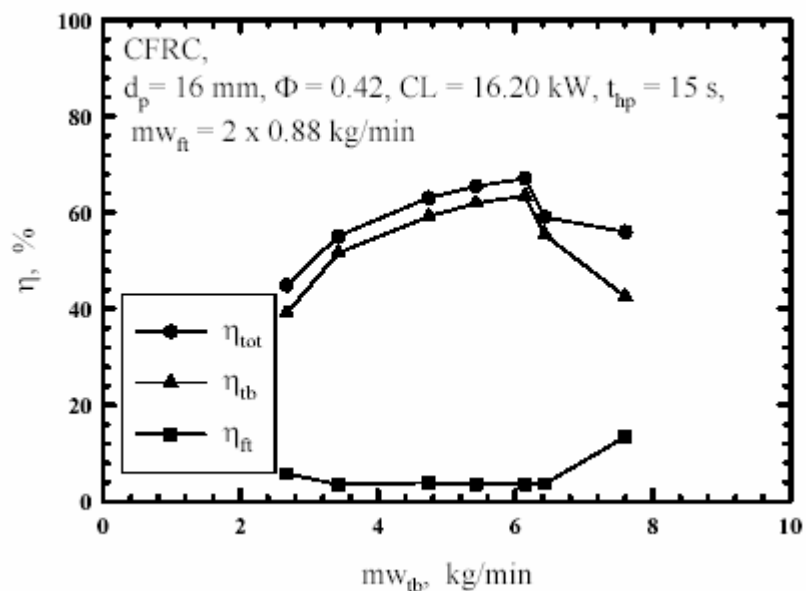


Figure 7. Effect of mw_{tb} on η .

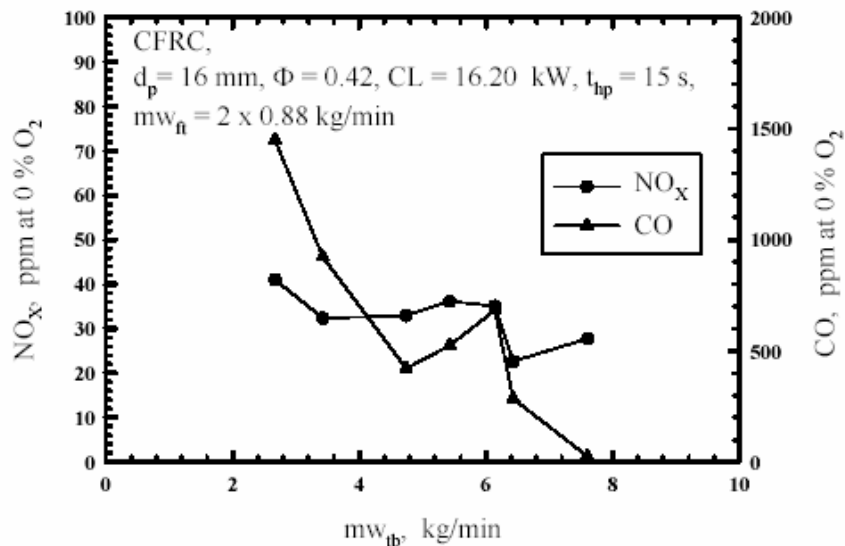


Figure 8. Effect of mw_{tb} on NO_x and CO.

3. Effect of thermal input CL.

To study the turndown ratio of the system, CL was increased from 8.08 kW up to 18.10 kW as shown in Figures 9 to 11. CL of more than 18.10 kW was not attempted due to excessively high temperature. As CL increases, T_{av} remarkably increases throughout the bed length except at the flame trap locations as shown in Figure 9. However, η_{tot} shows a decreasing trend as CL increases, as shown in Figure 10, because of the high heat loss through the combustor wall and through the exhaust gases with high velocity. Despite a significant increase in T_{av} with CL, almost insignificant changes to CO and NO_x emission were observed, as shown in Figure 11. Note that CO and NO_x emission of less than 30 ppm and 50

ppm, respectively, were yielded throughout the experimental range.

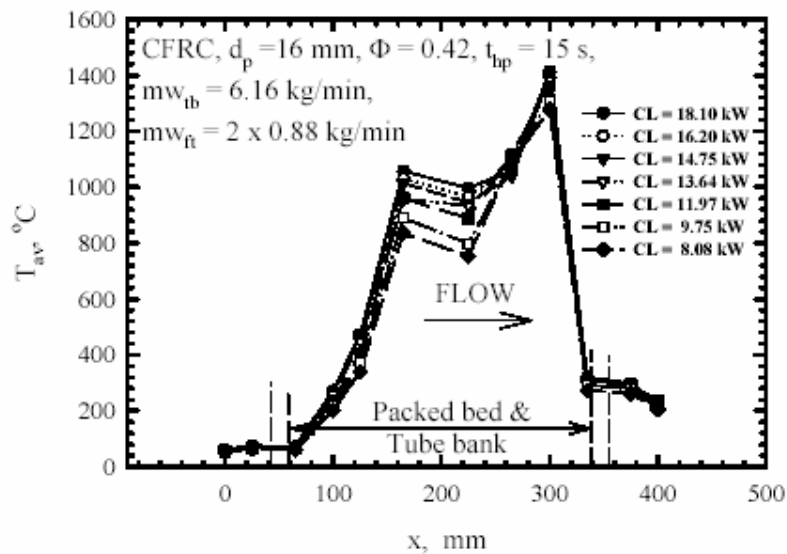


Figure 9. Effect of CL on time averaged temperature profiles T_{av} .

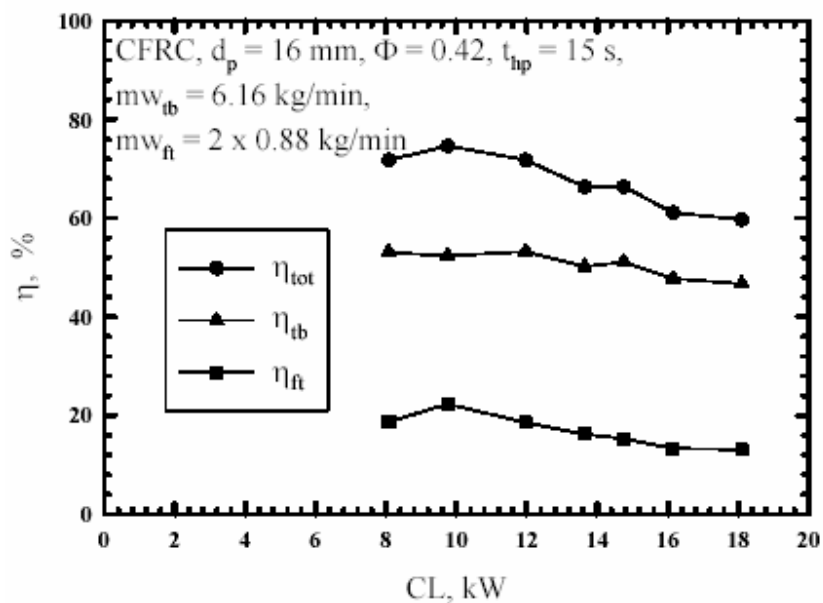


Figure 10. Effect of CL on η .

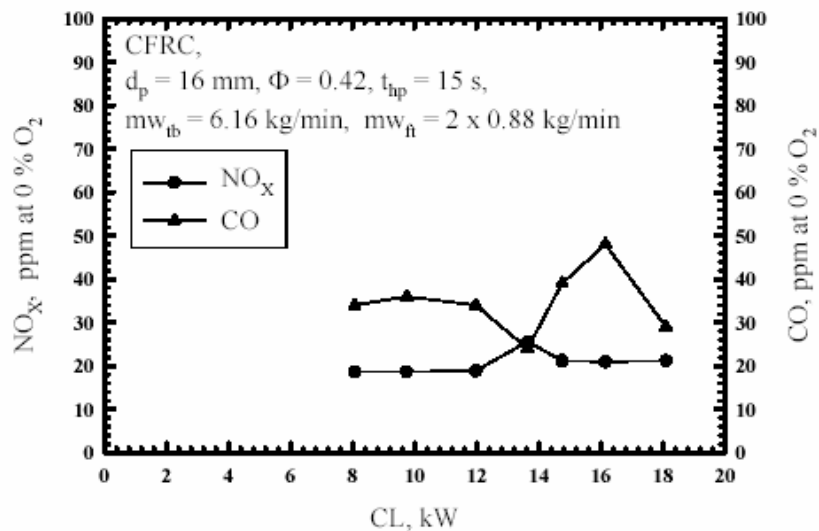


Figure 11. Effect of CL on CO and NO_x.

4. Comparison between the CFRC and the OWFC.

Because of the different nature in combustion characteristics, each system yields its own favorable experimental range. CFRC is suitable for relatively lean combustion, whereas OWFC is good for relatively rich combustion [3]. Therefore, a very narrow and common experimental range of the equivalence ratio Φ was permitted for comparison. Figure 12 shows a comparison of the temperature profiles between OWFC and CFRC at the same experimental conditions. $t_{hp} = 15$ s for CFRC is considered here without taking into account the same hot zone location as OWFC as suggested by Jugjai et al. [3]. CFRC yielded a higher maximum temperature and higher averaged temperature over the tube bank $(T_{av})_{CFRC}$ as compared with OWFC, assuring higher heat transfer performance and better emission characteristics as shown in

Figures 13 and 14 (see at $\Phi = 0.49$). At this $\Phi = 0.49$, CFRC yields almost double the η_{tot} , η_{tb} and η_{ft} with less CO and NO_x emission as compared with OWFC. Almost zero CO emission and NO_x of less than 30 ppm were observed for CFRC.

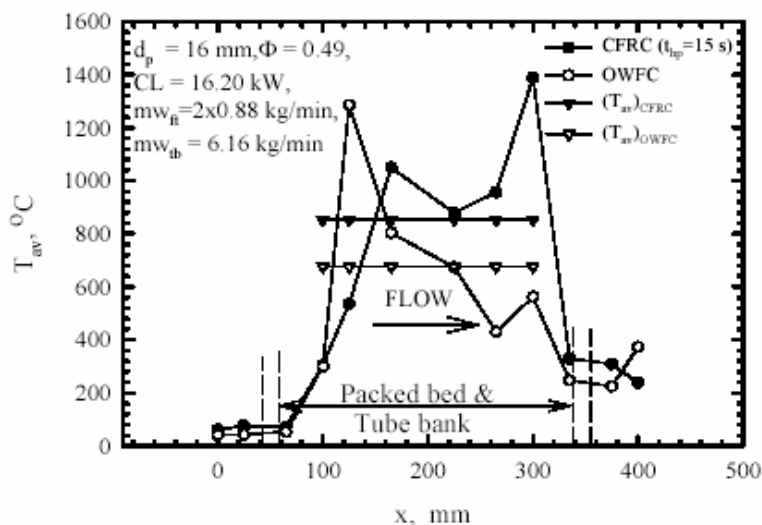


Figure 12. Comparison of typical T_{av} between the CFRC and the OWFC.

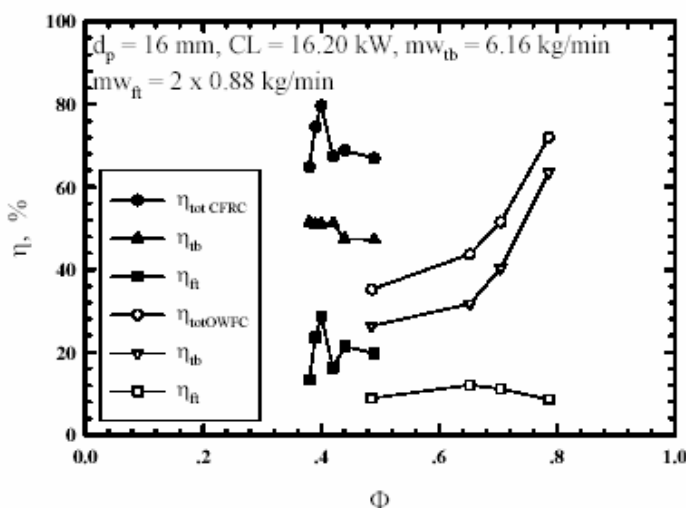


Figure 13. Comparison of η between the CFRC and the OWFC.

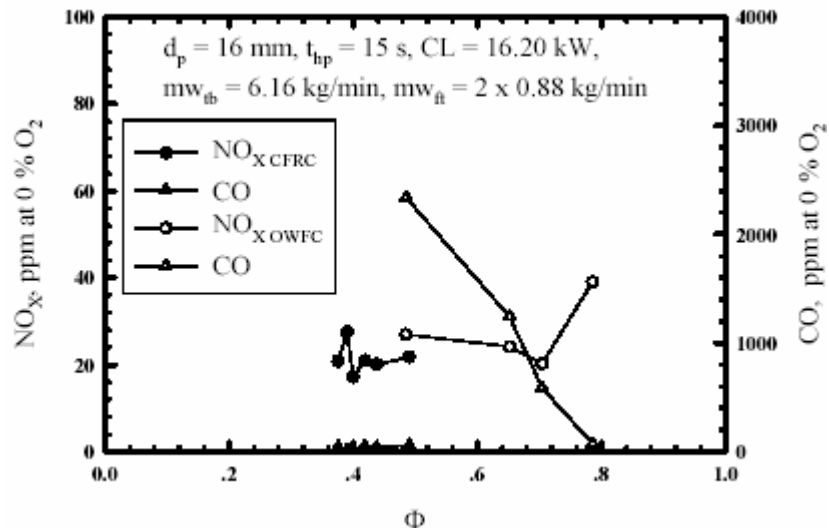


Figure 14. Comparison of CO and NO_x between the CFRC and the OWFC.

Conclusions

Successful development of the new SCH equipped with the CFRC technique has been carried out. Some important parameters have been investigated to improve performance of the new SCH.

- Flame traps play an important role in maintaining the boundary condition of the packed bed, whilst improving total thermal efficiency.
- Particle size has a dominant effect on temperature profile and thus thermal efficiency and emission characteristics. The particle size of $d_p = 16$ mm yielded the favorable

trapezoidal temperature profile, where the hot zone coincides with the tube bank.

- With the trapezoidal temperature profile, increasing the mass flow rate of the cooling water of the tube bank increases the thermal efficiency significantly with relatively low pollutant emissions of CO and NO_x. Too large a mass flow rate can cause an undesirable unsymmetrical temperature profile, which results in a shift in the hot zone far away from the tube bank and eventually a reduction in the thermal efficiency of the tube bank. Optimum mass flow rate of the cooling water of the tube bank was found to be 6.16 kg/min, yielding maximum thermal efficiency.
- Increasing the heat input appreciably increases the temperatures, but decreases the total thermal efficiency with remarkably low emissions of CO and NO_x (less than 50 ppm).
- At the same experimental condition, CFRC can yield almost twice as much thermal efficiency as OWFC, with much lower CO and NO_x emission (as low as 30 ppm). CFRC is suitable for relatively lean combustion, whereas OWFC is suitable for relatively rich combustion with comparable total thermal efficiencies and emission characteristics.

Nomenclature

CL	= heat input, kW
D_i	= inside diameter of tube, mm
D_o	= outside diameter of tube, mm
d_p	= average diameter of alumina pellets, mm
H	= bed height, mm
L	= bed length, mm
mw	= mass flow rate of the cooling water, kg/min
S_L	= longitudinal pitch, mm
S_T	= transverse pitch, mm
t_{hp}	= half-period, s
T	= temperature, K
T_w	= temperature of the cooling water, K
W	= bed width, mm

Greek Symbols

Φ	= equivalence ratio
η	= thermal efficiency

Subscripts

ft	= flame traps
i	= inlet
o	= outlet
tb	= tube bank or heat exchanger
tot	= total

References

- [1] Jugjai S. (2001) Experimental Study on Cyclic Flow Reversal Combustion in a Porous Medium, *Combust. Sci. and Tech.*, **163**, 245-260.
- [2] Xiong T.-Y., Khinkis M. J. and Fish F. F. (1995) Experimental study of a high-efficiency, low emission porous matrix combustor-heater, *Fuel*, **74**:11, 1641-1647.
- [3] Jugjai S., Wongveera S., Teawchaiitiporn T. and Limbwarnsin K. (2001) The Surface Combustor-Heater with Cyclic Flow Reversal Combustion, *Exp. Therm. Fluid Sci.*, **25**:3-4, 183-192.
- [4] Jugjai S., Sawananon A., Tongsuk K., Rungcharoen C. and Wachirawittayakul S. (2002) Presented at the 16th *Mechanical Engineering Network of Thailand (ME-NETT)*, Phuket, Thailand, pp. 229-234.